Numerical Simulation of Droplet Motion and Two-Phase Flow Field in an Oscillating Container

Tadashi Watanabe
Centre for Computational Science and e-Systems,
Japan Atomic Energy Agency,
Tokai-mura, Naka-gun, Ibaraki-ken, 319-1195, Japan
E-mail: watanabe.tadashi66@jaea.go.jp

ABSTRACT
The dynamic motion of the droplet in the oscillating flow field is simulated numerically using the arbitrary Lagrangian-Eulerian and level set coupled method. It is shown that radiating flows are generated from the droplet surface in the oscillating direction and the droplet moves toward the pressure node. The translational motion of the droplet is caused by the density variation, while the radiating flows are by the pressure variation. The flow field around the droplet in the oscillating container is found to be similar to that around the oscillating droplet in the stationary container.

Keywords: two-phase flow, droplet, oscillation, ALE method, level set method

1. INTRODUCTION

A levitated liquid droplet is used to measure material properties of molten metal at high temperature, since the levitated droplet is not in contact with a container, and the effect of container wall is eliminated for precise measurement [1]. The levitation of liquid droplet, which is also used for container-less processing of material, is controlled by using electromagnetic [2] electrostatic [3], or ultrasonic force [4] in the vertical direction. The levitated droplet is affected by an oscillating pressure field when the ultrasonic or acoustic levitator is used. Additionally, rotation is sometimes imposed on the droplet to stabilize its motion. The rotational motion is controlled by acoustic forces perpendicular to the vertical axis. It is thus important to know the behavior of droplet in an oscillating flow field. The streaming flows associated with ultrasonic levitator have been studied experimentally [5] and theoretically [6,7]. Although steady-state flows in and around the droplet were studied, the dynamic motion of the droplet in the oscillating flow field has not yet been discussed well.

The motion of the droplet and the flows around the droplet in an oscillating flow field are simulated numerically in this study. The oscillating flow field is modelled with an oscillating container, and the droplet is assumed to be levitated in the container. The oscillating flow field in the container is calculated using the arbitrary Lagrangian-Eulerian (ALE) method as a fluid-structure interaction problem, where the computational grid points for flow field are moved with the oscillating velocity of the container. The two-phase flow field is obtained using the level set method. In the level set method, the level set function, which is the distance function from the two-phase interface, is calculated by solving the transport equation using the local flow velocity. Incompressible Navier-Stokes equations are solved to obtain the flow field. The effect of compressibility is taken into account as the density perturbation. Sloshing phenomena are simulated first, and the results are compared

with an existing experiment for validation of the present numerical method. The motion of the droplet and the flow field around the droplet are simulated next, and characteristics of the oscillating flow fields and the effects of compressibility on the droplet motion are discussed.

2. GOVERNING EQUATIONS AND NUMERICAL METHOD

The level set method [8] is outlined briefly in the following. Governing equations for the droplet motion are the equation of continuity,

$$\nabla \cdot u = 0, \tag{1}$$

and the incompressible Navier-Stokes equations,

$$\rho \frac{\mathrm{D}u}{\mathrm{D}t} = -\nabla p + \nabla \cdot (2\mu D) - F_s, \tag{2}$$

where ρ, u, p and μ, respectively, are the density, the velocity, the pressure and the viscosity, D is the viscous stress tensor, and F_s is a body force due to the surface tension. The surface tension force is given by

$$F_s = \sigma \kappa \delta \nabla \phi, \tag{3}$$

where σ, κ, δ, and ϕ, are the surface tension, the curvature of the interface, the Dirac delta function and the level set function, respectively. The level set function, which is the normal distance from the interface, is defined as $\phi = 0$ at the interface, $\phi < 0$ in the liquid region, and $\phi > 0$ in the gas region. The curvature is expressed in terms of ϕ:

$$\kappa = \nabla \cdot \left(\frac{\nabla \phi}{|\nabla \phi|}\right). \tag{4}$$

The density and viscosity are given by

$$\rho = \rho_l + (\rho_g - \rho_l) H \tag{5}$$

and

$$\mu = \mu_l + (\mu_g - \mu_l) H \tag{6}$$

where the subscripts g and l denote the gas and liquid phase, respectively, and H is a Heaviside-like function defined by

$$H = \begin{cases} 0 & (\phi < -\varepsilon) \\ \frac{1}{2}\left[1 + \frac{\phi}{\varepsilon} + \frac{1}{\pi}\sin\left(\frac{\pi\phi}{\varepsilon}\right)\right] & (-\varepsilon \le \phi \le \varepsilon) \\ 1 & (\varepsilon < \phi) \end{cases}, \tag{7}$$

where ε is a small positive constant for which $|\nabla \phi| = 1$ for $|\phi| \le \varepsilon$. The evolution of ϕ is given by

$$\frac{\mathrm{D}\phi}{\mathrm{D}t} = 0, \tag{8}$$

In this study, the ALE method [9] is applied, and the computational grid is moved with the same velocity as the velocity of the oscillating container. The substantial derivative terms in Eqns (2) and (8) are thus defined by

$$\frac{\mathrm{D}}{\mathrm{D}t} = \frac{\partial}{\partial t} + (u - U)\cdot\nabla \tag{9}$$

where U is the velocity of the computational grid.

In order to maintain the level set function as a distance function, an additional equation is solved:

$$\frac{\partial \phi}{\partial \tau} = (1 - |\nabla\phi|)\frac{\phi}{\sqrt{\phi^2 + \alpha^2}}, \tag{10}$$

where τ and α are an artificial time and a small constant, respectively. The level set function becomes a distance function in the steady-state solution of the above equation. The following equation is also solved to preserve the total mass in time [10]:

$$\frac{\partial \phi}{\partial \tau} = (A_o - A)(1 - \kappa)|\nabla\phi|, \tag{11}$$

where A_0 denotes the total mass for the initial condition and A denotes the total mass corresponding to the level set function. The total mass is conserved in the steady-state solution of the above equation.

The effect of compressibility is taken into account simply as the density perturbation, since the amplitude of pressure variation and thus the density variation are both small in this study. The density perturbation is defined by

$$\delta\rho = \delta p / c^2, \tag{12}$$

where c is the sound speed.

The finite difference method is used to solve the governing equations. The staggered mesh system is applied for spatial discretization of velocities. The convective terms are discretized using the second order upwind scheme and other terms by the second order central difference scheme. Time integration is performed by the second order Adams-Bashforth method. The SMAC method [11] is used to obtain pressure and velocities. The Poisson equation for pressure correction is solved using the Bi-CGSTAB method. The domain decomposition technique is applied and the message passing interface (MPI) library is used for parallel numerical simulations. The block Jacobi preconditioner [12] is used and the simulations are performed using parallel computer systems.

3. RESULTS AND DISCUSSION

3.1. SLOSHING ANALYSIS FOR VALIDATION OF NUMERICAL METHOD

Liquid sloshing in a rectangular tank is simulated first as a sample problem for validation of the present numerical method using the ALE and level set coupled method. The simulation conditions are the same as the conditions of the sloshing experiment [13]. The two-dimensional phenomena are dominant in the experiment, and the simulation is performed in two dimensions. The size of the tank is 0.57 m × 0.3 m and the initial water level is 0.15 m as shown in Figure 1. Variations of liquid level are observed at three locations: Probe 2 near

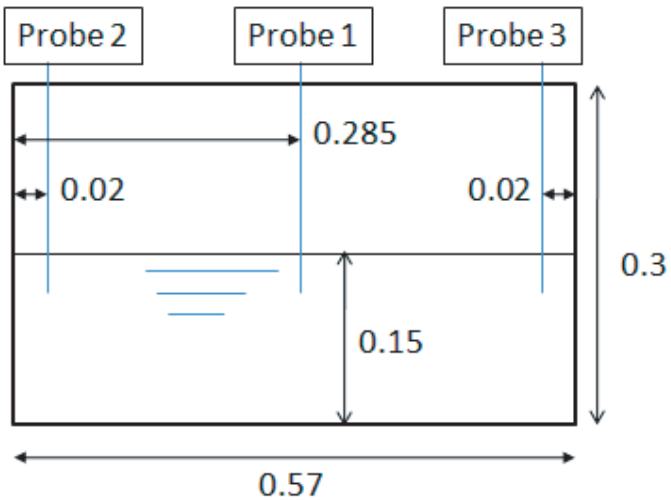

Figure 1 Sketch of sloshing experiment.

the left wall, Probe 1 at the center, and Probe 3 near the right wall. Properties of water and air at the room temperature and atmospheric pressure are used. The number of mesh cells is 190 × 100, and the time step size is 0.001 s. The tank is set in an oscillatory motion in horizontal direction. The oscillation of the tank location in the horizontal direction is given by

$$x = A\sin(\omega t), \tag{13}$$

where A = 0.005 m and ω = 6.0578 rad/s are, respectively, the amplitude and the angular frequency of the oscillation. The velocity of the oscillating tank is used in the simulation and is given as the differential of the tank location,

$$U = A\omega\cos(\omega t). \tag{14}$$

Time evolutions of the liquid level are shown in Figure 2. The simulated results are compared with the experimental data obtained at Probe 2, Probe 1 and Probe 3, in Figures 2 (a), (b) and (c), respectively. The frequency of the liquid level oscillation is the same as that of the tank oscillation, and the amplitude of the liquid level oscillation is increased with time. The sloshing phenomena are thus simulated well under the experimental conditions. The agreement between the simulation and the experiment is shown to be satisfactory. It is found that not only the large variations near the side walls but also the small variation in the center of the tank are predicted very well. It is thus demonstrated that the present numerical method using the ALE and level set coupled method works very well for simulating two-phase flow filed in an oscillating container.

3.2. DROPLET MOTION

The dynamic motion of the droplet in an oscillating flow field is simulated next. The oscillating flow field is modelled with the oscillating container, and the droplet is assumed to be levitated in the center of the container as shown in Figure 3. Water and air properties are assumed. Vertical and horizontal sizes of the container are 0.017 m and 0.01 m, respectively, and the radius of the droplet is 0.002 m. The container is oscillated in the vertical direction with the frequency of 20 kHz and the sound pressure of 0.25 kPa. The

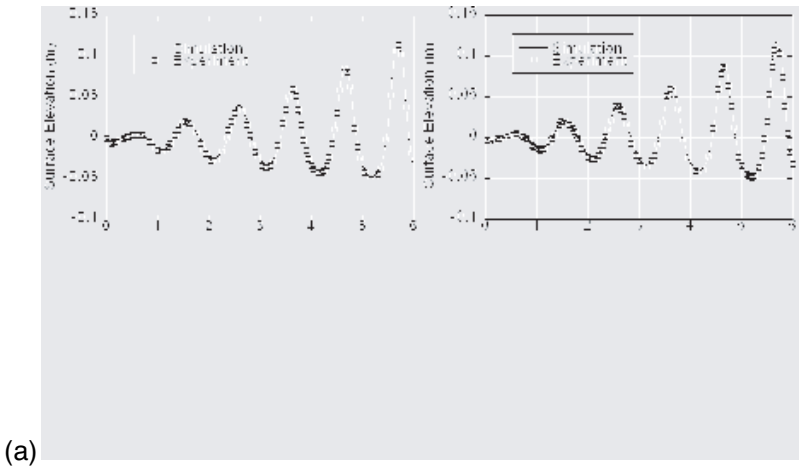

(a)

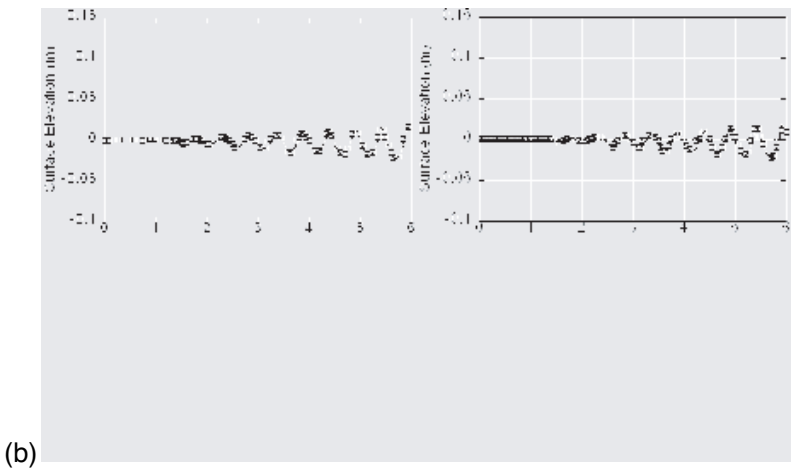

(b)

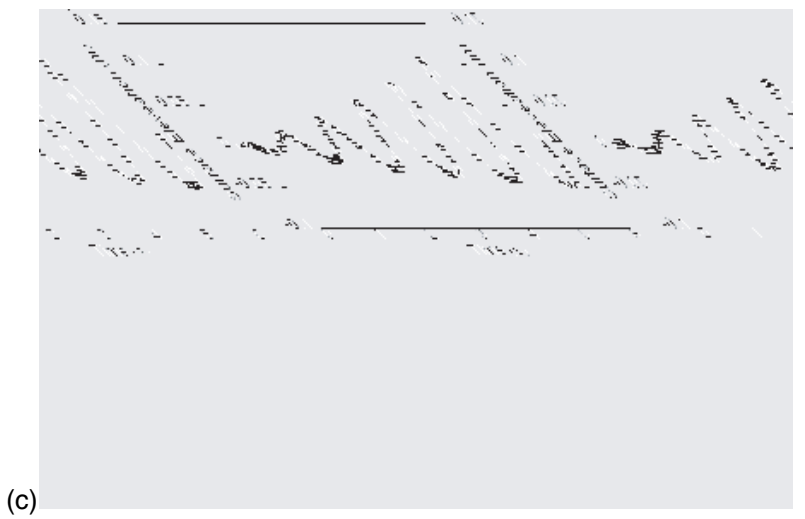

(c)

Figure 2 Evolution of surface elevation: (a) Probe2, (b) Probe1, (c) Probe3.

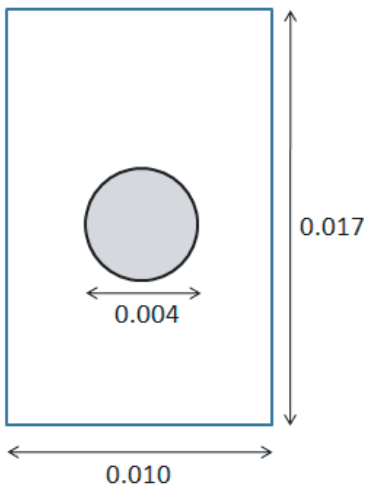

Figure 3 Droplet in an oscillating container

sound speed is about 340 m/s in the air, and the vertical size corresponds to half the wave length. This region size is sufficient to simulate the pressure variation around the droplet. The gravitational acceleration is not included. The number of mesh cells is 170 × 100, and the time step size is 1×10^{-6} s.

Simulated pressure fields in the oscillating container without the droplet are shown in Figure 4, where the vertical position is the distance from the center of the container. The pressure distributions in the vertical direction are shown in every 0.1T, where T is the oscillation period of the container. The pressure node, at which the pressure variation becomes zero, is set at the center of the container in (a), while at the bottom in (b). It is shown that the pressure distribution is oscillated around the pressure node, and the oscillation frequency is the same as that of the oscillating container. The pressure distribution is almost linear in Figure 4, since the compressibility is taken into account as the pseudo compressibility defined by Eqn (12). This is, however, sufficient to simulate the pressure field around the droplet with the radius of 0.002 m.

The dynamic motion of the droplet in the oscillating pressure field is shown in Figure 5. The droplet position and the velocity field are shown in every 0.05 s. The position of the pressure node is set at the center, bottom, and top in Figures 5 (a), (b) and (c), respectively. In any cases, radiating flows in the vertical upward and downward directions are generated from the surface of the droplet in the early stage. This is corresponding to the experimental observation [5]. In the case with the pressure node at the center, the droplet stays at the initial position, and symmetric vortices grow around the droplet. In the case with the pressure node at the bottom or top, the droplet moves gradually from the initial position toward the pressure node. It is shown that the radiating flow velocity becomes larger in front of the droplet in these cases. The radiating flows are still seen in the rear side, though the velocity becomes smaller.

The time evolutions of the droplet position are shown in Figure 6, where the top position of the droplet is depicted for three cases with different positions of the pressure node. It is shown that the droplet is accelerated from the very early stage, and the translational velocity increases for the cases with the pressure node at the bottom or top. The simulation region is not so large in our simulations, and the moving droplets hit the bottom or top boundaries in

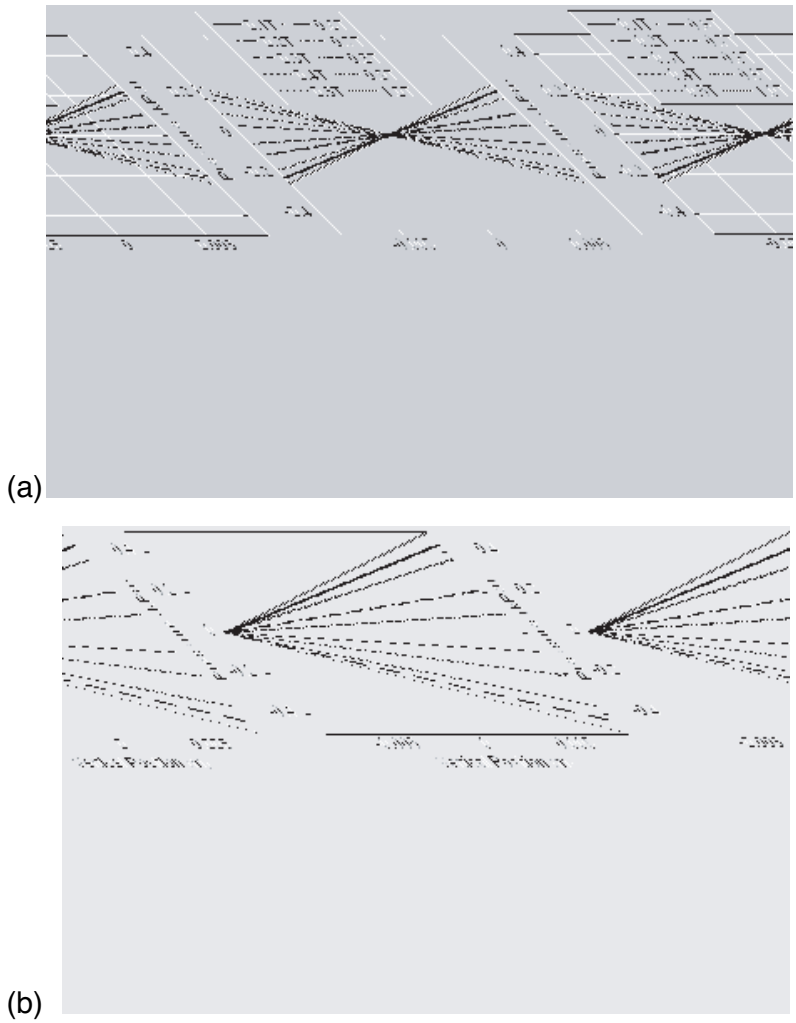

Figure 4 Pressure variation in one oscillation period T: (a) pressure node at the center, (b) pressure node at the bottom.

the later stage as indicated in Figures 5 (b) and (c). For the case with the pressure node at the center, the droplet does not move for a long time, though finally being affected by the flow field developed in the container as shown in Figure 5 (a). It is found from Figures 5 and 6 that the droplet stays stably at the pressure node in the oscillating pressure field.

In order to see clearly the oscillating flow field around the droplet, the droplet is fixed at the center in Figure 7 (a) for the case with the pressure node at the center. It is shown that the radiating flows from the droplet surface in the vertical direction are larger than those shown in Figure 5 (a) for the free droplet. It is thus found that the induced flow field is qualitatively the same but quantitatively different for the fixed droplet and the free droplet. The net momentum from the oscillating container to the radiating flow is larger for the fixed droplet, since the free droplet moves slightly in the oscillating flow field, even though it stays stably at the initial position.

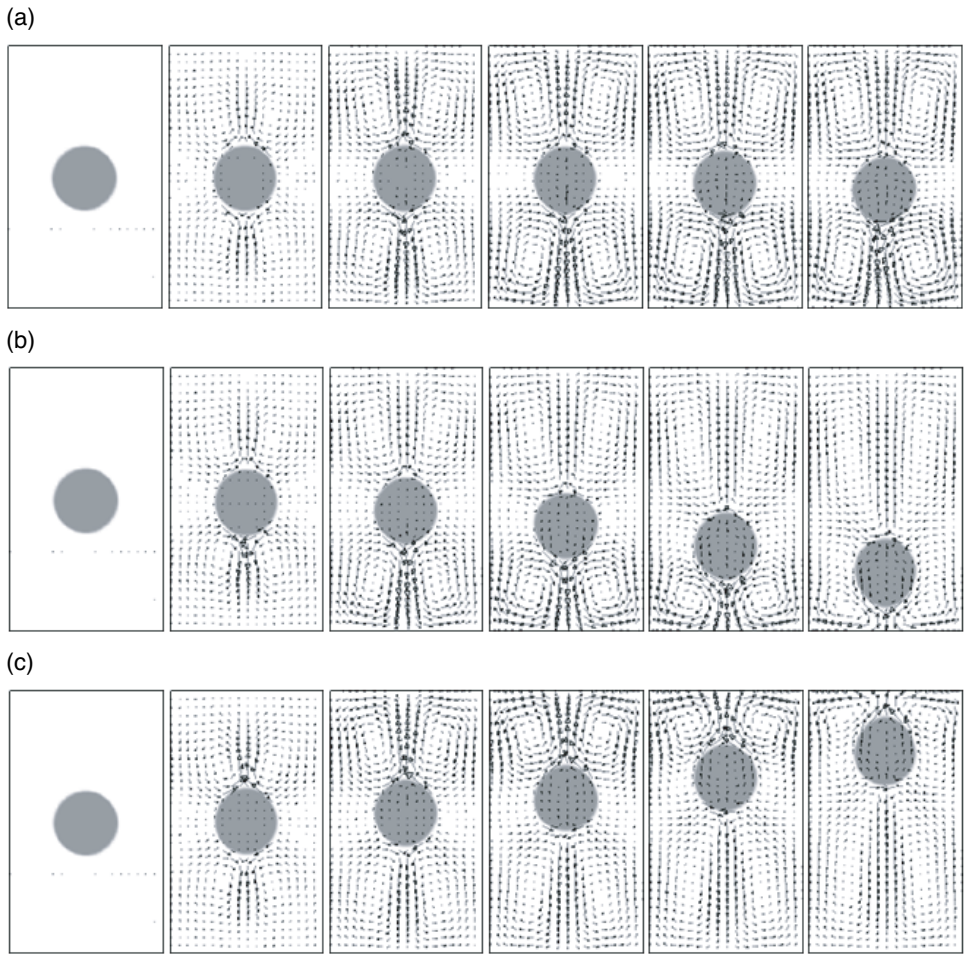

Figure 5 Flow fields in every 0.05 s: (a) pressure node at the center, (b) pressure node at the bottom, (c) pressure node at the top

In Figure 7 (b), the flow field around the oscillating droplet is shown for comparison. The container is fixed, and the velocity of the ALE grid is zero, but the droplet is oscillated in the vertical direction with the same amplitude and frequency as those for Figure 7 (a). Although the flow field is not symmetric for upward and downward directions, the radiating flows from the droplet surface are still seen in the vertical direction. The radiating flow from the oscillating body is well known [14], and the similar flow is also known for the fixed body in the oscillating pressure field [5]. It is thus found that these flow fields are both simulated well in Figures 7 (a) and (b). Net momentum from the oscillating motion to the flow field is smaller for the case with oscillating droplet than for the case with oscillating container, and the magnitude of radiating flow is smaller in Figure 7 (b). It is noted that the initial position of the oscillating droplet is not at the center of the simulation region, since the oscillating droplet has the maximum velocity at the center and zero velocity at the highest and lowest positions. The flow field is thus not symmetric in Figure 7 (b).

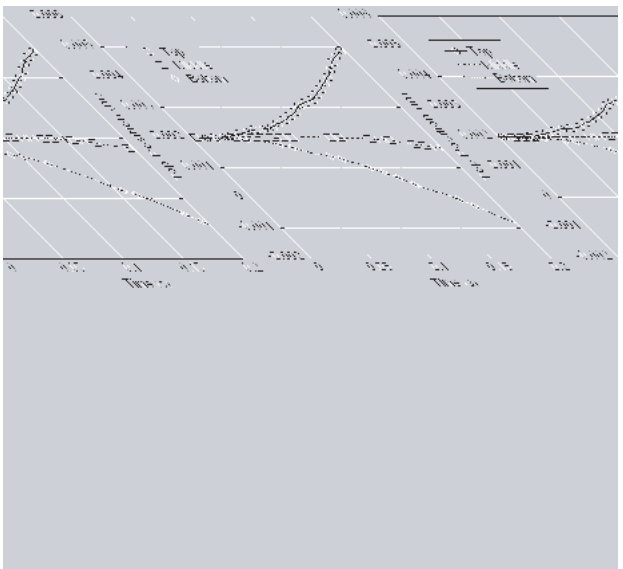

Figure 6 Variation of droplet position with different pressure node

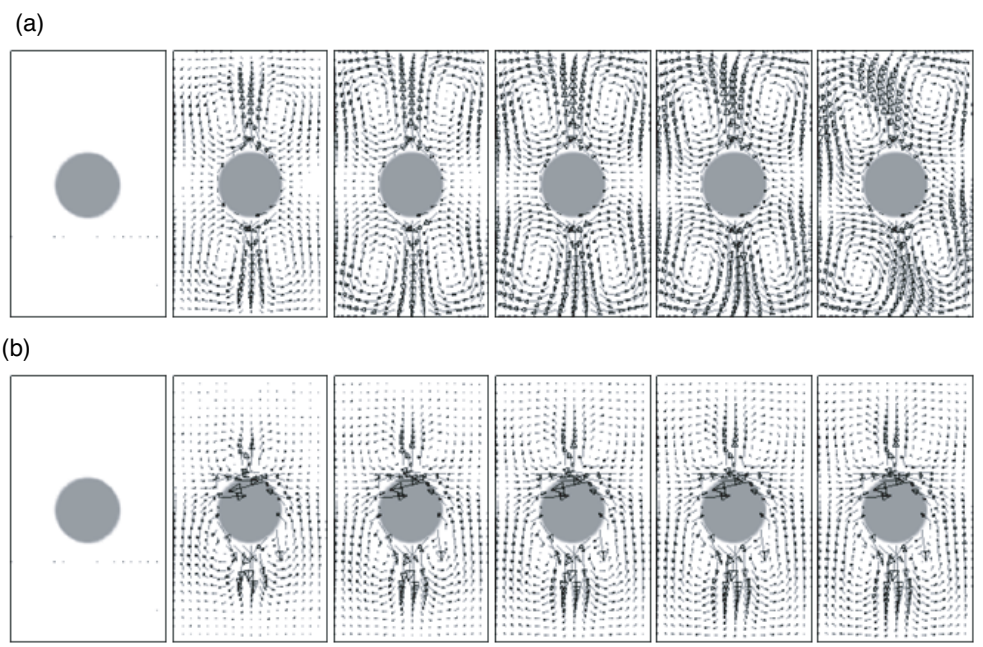

Figure 7 Comparison of oscillating flow fields: (a) fixed droplet with oscillating container, (b) oscillating droplet with fixed container.

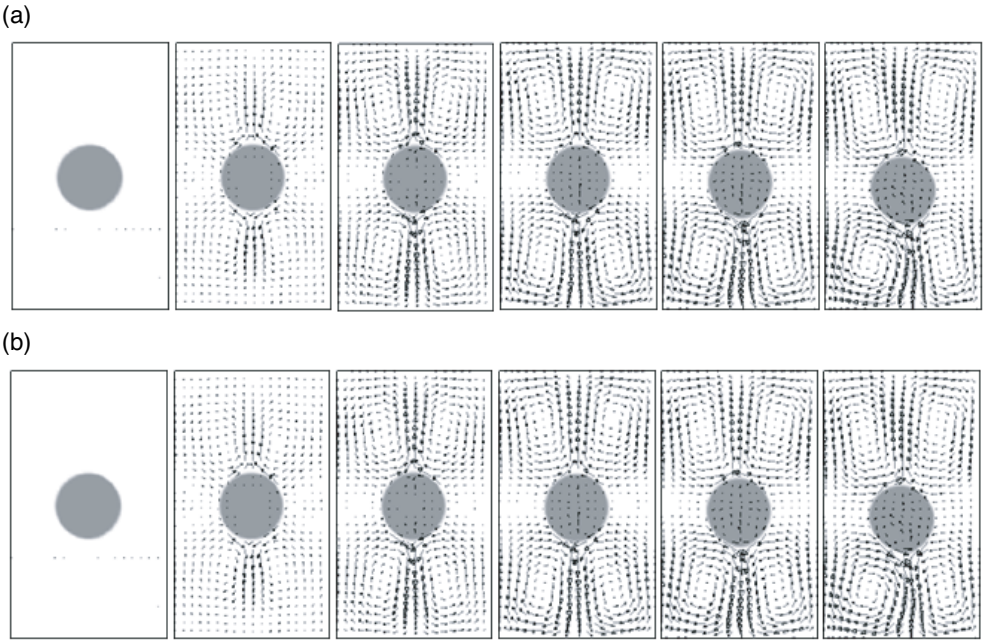

Figure 8 Incompressible flow fields: (a) pressure node at the bottom, (b) pressure node at the top.

The effect of compressibility is shown in Figure 8. The pseudo compressibility defined by Eqn (12) is assumed in our simulations, but this effect is not taken into account in Figure 8. The position of the pressure node is set at the bottom for Figures 8 (a) and top for (b), respectively. The droplet is not fixed and freely movable according to the flow field. It is shown in Figures 8 (a) and (b) that almost the same radiating flows are generated, and the droplet stays at the initial position. The flow fields are similar to that in Figure 5 (a). The forces acting on the droplet are balanced between upper and lower surfaces in Figure 5 (a), and the droplet stays at the initial position. The droplet moves toward the pressure node in the pseudo compressible cases as shown in Figures 5 (b) and (c), since the net force on the droplet is affected by the position of the pressure node. In the incompressible case, however, the net force on the droplet is not affected by the pressure node. The net force on the droplet is composed of the effects of the pressure variation and the density variation. The pressure variation for the incompressible case is the same as that for the pseudo compressible case, but the density variation is included only in the pseudo compressible case. The density variation is thus found to be important for the translational motion of the droplet. It is also found that the radiating flows are generated only by the pressure variation.

4. CONCLUSION

The dynamic motion of the droplet and the flows around the droplet in the oscillating flow field have been simulated numerically in this study. The oscillating flow field was modelled with an oscillating container using the ALE method as a fluid-structure interaction problem, and the two-phase flow field was obtained using the level set method. Sloshing phenomena were simulated first for validation of the present numerical method, and the excellent agreement between the simulation and the experiment was shown. The motion of the droplet

in the oscillating container was simulated next. The radiating flows from the droplet surface were shown to be generated in the oscillating direction. The droplet moved toward the pressure node, and stayed stably at the pressure node. The translational motion of the droplet was caused by the density variation, while the radiating flows were by the pressure variation. The flow field around the droplet in the oscillating container was found to be similar to that around the oscillating droplet in the stationary container. It was demonstrated in this study that oscillating two-phase flow fields including free surface or droplet could be simulated well by the ALE and level set coupled method.

REFERENCES

[1] Egry, I., Lohoefer, G. and Jacobs, G., Surface Tension of Liquid Metals: Results from Measurements on Ground and in Space, *Physical Review Letters*, 1995, 75, 4043-4046.

[2] V. Shatrov, V., Priede, J. and Gerbeth, G., Three-Dimensional Linear Stability Analysis of the Flow in a Liquid Spherical Droplet driven by an Alternating Magnetic Field, *Physics of Fluid*, 2003, 15, 668-678.

[3] Rhim, W.K. and Chung, S. K., Isolation of Cystallizing Droplets by Eectrostatic Lvitation, *Methods:A Companion to Methods in Enzymology*, 1990, 1, 118-127.

[4] Yarin, A. L., Weiss, D. A., Brenn, G. and Rensink, D., Acoustically Levitated Drops: Drop Oscillation and Break-Up Driven by Ultrasound Modulation, *Journal of Multiphase Flow*, 2002, 28, 887-910.

[5] Trinh, E. H. and Robey, J. L., Experimental Study of Streaming Flows Associated with Ultrasonic Levitators, *Physics of Fluid*, 1994, 6, 3567-3579

[6] Yarin, L. L., Brenn, G., Keller, J., Pfaffenlehner, M, Ryssel, E. and Tropea, C., Flowfield Characteristics of an Aerodynamic Acoustic Levitator, *Physics of Fluid,* 1997, 9, 3300-3314.

[7] Rednikov, A. Y., Zhao, H., Sadhal, S. S. and Trinh, E. H., Steady Streaming Around a Spherical Drop Displaced from the Velocity Antinode in an Acoustic Levitation Field, *Journal of Acoustic Society of America,* 1999, 106, 3289-3295.

[8] Sussman, M. and Smereka, P., Axisymmetric free boundary problems, *Journal of Fluid Mechanics,* 1997, 341, 269-294.

[9] Hirt, C. W., Amsden, A. A. and Cook, J. L., An arbitrary Lagrangian-Eulerian computing method for all flow speeds, *Journal of Computational Physics,* 1974, 14, 227–253.

[10] Chang, Y. C., Hou, T. Y., Merriman, B. and Osher, S., A level set formulation of Eulerian interface capturing methods for incompressible fluid flows, *Journal of Computational Physics,* 1996, 142, 449-464.

[11] Amsden, A. A. and Harlow, F. H., A simplified MAC technique for incompressible fluid flow calculations, *Journal of Computational Physics.,* 1970, 6, 322-325.

[12] Benzi, M., Preconditioning techniques for large linear systems: a survey, *Journal of Computational Physics.,* 2002, 182, 418-477.

[13] Liu, D. and Lin, P. A Numerical Study of Three-Dimensional Liquid Sloshing in Tanks, *Journal of Computational Physics,* 2008, 227, 3921-3939.

[14] Schlichting, H., *Boundary-Layer Theory,* 7th edn., McGraw Hill, New York, 1979, 428-432.